AD-A103 901 HOWARD UNIV WASHINGTON D C DEPT OF CHEMISTRY F/G 7/4
OVERTONE VIBRATIONS OF OH GROUPS IN FUSED SILICA OPTICAL FIBERS--ETC(U)
SEP 81 J STONE, G E WALRAFEN N00014-80-C-0305
UNCLASSIFIED TR-4 NL

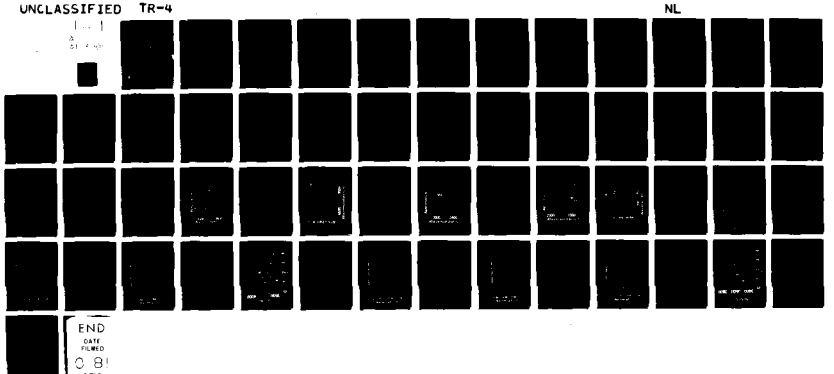

END
DATE FILMED
0 81
DTIC

SECURITY CLASSIFICATION OF THIS PAGE (When Data Entered)

REPORT DOCUMENTATION PAGE	READ INSTRUCTIONS BEFORE COMPLETING FORM
1. REPORT NUMBER: 4	2. GOVT ACCESSION NO.: AD-A103 901
3. RECIPIENT'S CATALOG NUMBER: (1) TR-4	
4. TITLE (and Subtitle): Overtone Vibrations of OH Groups in fused Silica Optical Fibers.	5. TYPE OF REPORT & PERIOD COVERED: Technical Report #4, 1981
	6. PERFORMING ORG. REPORT NUMBER
7. AUTHOR(s): J. Stone and G. E. Walrafen	8. CONTRACT OR GRANT NUMBER(s): N00014-80-C-0305
9. PERFORMING ORGANIZATION NAME AND ADDRESS: Chemistry Department, Howard University, Washington D. C. 20059	10. PROGRAM ELEMENT, PROJECT, TASK AREA & WORK UNIT NUMBERS: NR 051-733
11. CONTROLLING OFFICE NAME AND ADDRESS: Office of Naval Research, Arlington, Va 22217	12. REPORT DATE: September 1981
	13. NUMBER OF PAGES: 15
14. MONITORING AGENCY NAME & ADDRESS(if different from Controlling Office)	15. SECURITY CLASS. (of this report)
	15a. DECLASSIFICATION/DOWNGRADING SCHEDULE

LEVEL

16. DISTRIBUTION STATEMENT (of this Report)

Approved for public release: Distribution unlimited

DTIC ELECTE SEP 8 1981 H

17. DISTRIBUTION STATEMENT (of the abstract entered in Block 20, if different from Report)

18. SUPPLEMENTARY NOTES

19. KEY WORDS (Continue on reverse side if necessary and identify by block number)

Overtone, Vibrations of OH Groups, Fused Silica Optical Fibers

less than greater than 1000

20. ABSTRACT (Continue on reverse side if necessary and identify by block number)

The OH-stretching fundamental, and ~~the first, second and third OH overtone~~ vibrations have been examined using pure and GeO_2 - doped graded index, fused silica optical fibers having OH contents from 1ppm to ~~10~~ 18 ppm. The previously reported component substructure of the fundamental vibrations of fused silica. Several new vibrations were uncovered and assigned. Examinations of deuterated OH samples helped to verify the assignments. The spectral broadening produced by GeO_2 was interpreted in terms of a wider range of enviroments seen by the OH oscillators, compared to pure fused silica.

DD FORM 1 JAN 73 1473 EDITION OF 1 NOV 65 IS OBSOLETE S/N 0102-014-6601

SECURITY CLASSIFICATION OF THIS PAGE (When Data Entered)

1 / 1

AD A103901

DTIC FILE COPY

81 9 08 62

FINAL AS SENT TO JOURNAL 1/13/81

"Overtone Vibrations of OH Groups in Fused Silica Optical Fibers"

by

J. Stone
Bell Laboratories
Crawford Hill Laboratory
Holmdel, New Jersey 07733

and

G. E. Walrafen
Chemistry Department
Howard Universtiy
Washington, DC 20059

ABSTRACT

The OH-stretching fundamental, and the first, second, and third OH overtone vibrations have been examined using pure, and GeO_2-doped graded index, fused silica optical fibers having OH contents from <1 ppm to $>10^2$ ppm. The previously reported component substructure of the fundamental OH-stretching contour was found to be repeated in the overtones, along with a set of combinations involving fundamental vibrations of fused silica. Several new vibrations were uncovered and assigned. Examinations of deuterated OH samples helped to verify the assignments. The spectral broadening produced by GeO_2 was interpreted in terms of a wider range of environments seen by the OH oscillators, compared to pure fused silica.

1. Introduction

The overtone vibrations of the OH group in fused silica, particularly the first overtone, are of considerable practical importance because they give rise to transmission losses in long optical fibers.[1] The OH-stretching overtones are also of interest from a fundamental point of view because they provide evidence relating to bonding and structure in fused silica[2] as well as in other glasses.[3,4,5]

When water is incorporated into fused silica, silanol groups, Si-OH, are formed,[6] as opposed to the discrete H_2O molecules found in crystalline quartz.[7] Further, the vibrational frequencies of the OH groups in fused silica are sensitive to the surrounding environment because the OH vibrations are decoupled dynamically from the Si versus OH vibrations. The fundamental OH-stretching vibrations occur within the 3000-4000 cm^{-1} region, whereas the Si versus OH stretching occurs near 970 cm^{-1}.[6] This environmental sensitivity leads to structured fundamental and overtone OH-stretching contours in both the infrared and Raman spectra, the analysis of which provides an understanding of the structure and properties of the wet glass.

Examination of the shapes of the fundamental Raman and infrared OH-stretching contours from pure fused silica indicates the presence of substructure. The maximum Raman and infrared intensities occur at 3690 cm^{-1} and 3665 cm^{-1},[2,8] respectively, and each spectrum shows a shoulder near 3610 cm^{-1};[2,8] there is also a maximum in the depolarization ratio near 3620 cm^{-1}.[8] These observations constitute definite physical evidence for three OH-stretching components near 3690 cm^{-1}, 3665 cm^{-1}, and 3610 cm^{-1}. Further, decomposition of the Raman and infrared OH-stretching contours into Gaussian components indicates a fourth broad, weak component near 3510 cm^{-1}.[2] The component substructure should thus also be evident in the overtones, although complications due to anharmonicity, or to combinations, etc., are to be expected. (The detailed nature of the interactions leading to the four OH-stretching components has been described previously,[2] and will not be

considered here.)

In this work we have examined the first, second, and third OH-stretching overtones in long lengths of fused silica optical fibers, and re-examined the fundamental region for thick silica samples, both deuterated and undeuterated. We also have obtained the Raman spectrum of the first OH-stretching overtone, which is extremely weak.

The picture that emerges is one in which the fundamental contour consists of three or four OH-stretching components, plus several combination tones. These features are repeated in the substructure of the first three overtones, and can be identified in slightly modified form in the OH overtone substructure of GeO_2-doped silica. Several weak features of the absorption spectra, some previously unreported, are explained. Also, we observed a resolved absorption maximum in a deuterated sample which may arise from a combination mode which is unresolved in the undeuterated spectrum. The details of the present fundamental and overtone observations and assignments follow.

2. Experimental

Fundamental infrared absorbance spectra in the range of 600 to 4950 cm^{-1} were obtained from samples of Suprasil-2, Spectrasil, and Amersil TO-8, and also from samples of the same materials in which the OH was partially deuterated by $OH \rightleftharpoons OD$ exchange.[9] The OH content of the undeuterated samples ranged from about 10^2 to 10^3 ppm. The absorbance spectra were obtained with a Nicolet 7000 Fourier transform infrared (FTIR) instrument. Each absorbance spectrum is the Fourier transform of an average of 128 interferograms. FTIR difference spectra were also obtained from linear combinations of deuterated and undeuterated absorbance spectra.

Deuterated samples of Suprasil-2, Spectrasil, and TO-8 in the form of rods ~1 cm in diameter were obtained by $OH \rightleftharpoons OD$ exchange. The rods were heated for 5 days at 1000°C in a D_2 atmosphere to produce the isotopic exchange. However, because the deuteration was not complete, a small fraction of the original OH remained. The deuterated rods were then cut

into appropriate lengths and the ends were optically polished.

In order to observe the OH-stretching overtone spectra, it was necessary to use very long sample lengths. This was accomplished by the use of optical fibers. Appropriate lengths were used depending on the OH content of the silica, and the overtone under study. (The maximum absorbances per cm of the OH-stretching fundamental and overtones are: fundamental, 10^{-2}/ppm OH; first overtone, 5×10^{-5}/ppm OH, second overtone, 10^{-6}/ppm OH; and, third overtone, 10^{-7}/ppm OH.)[9] Fibers of Spectrasil ($>10^3$ ppm OH), Suprasil ($>10^3$ ppm OH), and Amersil TO-8 ($>10^2$ ppm OH) were made by drawing silica rods to a diameter of 125 μm in an electric furnace. A protective coating of Nylon was added immediately after drawing. The GeO_2-doped silica fibers were graded-index multimode, or step-index single-mode core, silica-clad fibers, with plastic outer coating of the type commonly used in fiber optics research.[10] The light-guiding core of the graded-index fiber has a GeO_2 concentration varying from about 14 percent at the center, to zero at the core-cladding boundary (parabolic profile). Thus its absorption spectrum represents a weighted average of those from pure silica to 14 percent GeO_2. The core of the single-mode fiber is uniformly doped with about 5 percent GeO_2.

When light propagates in a low-loss optical fiber, attenuation in the spectral regions of the OH-stretching overtones results mainly from the overtone absorption--the attenuation from Rayleigh scattering is relatively small. When light enters the core of an optical fiber, the decrement in the light power spectrum $I_L(\lambda)$ is given by

$$dI_L(\lambda) = -[\alpha_a(\lambda) + \alpha_s(\lambda)]I_L(\lambda)dL \ , \qquad (1)$$

where $\alpha_a(\lambda)$ is the absorption loss coefficient, $\alpha_s(\lambda)$ is the scattering loss coefficient, and λ is the wavelength. Then

$$I_{L_2}(\lambda) = I_{L_1}(\lambda) e^{-[\alpha_B(\lambda) + \alpha_S(\lambda)](L_2 - L_1)} \tag{2}$$

and

$$\alpha_B(\lambda) + \alpha_S(\lambda) = \frac{1}{L_2 - L_1} \ln \frac{I_{L_1}(\lambda)}{I_{L_2}(\lambda)} \ , \tag{3}$$

where L_1 and L_2 are fiber lengths for which the emergent light is measured (for a fixed light input). Because $\alpha_B(\lambda)$ and $\alpha_S(\lambda)$ are additive, the absorbance contour can be taken as the portion of the attenuation spectrum above the background scattering curve. In the present work a tungsten-halogen lamp was employed as a light source. Spectra were obtained with a Jarrell-Ash 0.25 m monochromator; we determined that the resulting spectral shapes were not limited by the low instrumental resolution. Because the absorbance measurement performed here is a ratio measurement, it is independent of factors related to the spectral sensitivity of the measurement system.

Raman spectra of the first OH-stretching overtone region were also obtained using 20 to 115 m of pure fused silica fiber having OH contents ranging from about 500-1300 ppm. Interference-filtered argon ion laser radiation at 488.0 nm was used for excitation, with an Instruments S.A. HG2S holographic grating double monochromator having enhanced red sensitivity. The overtone Raman spectra were extremely weak, however, and yielded data of limited value.

Infrared fundamental and overtone contours were decomposed into Gaussian components using a DuPont 310 analog computer.

3. *Experimental Results*

A. Infrared Fundamental OH- and OD-Stretching Region

FTIR absorbance spectra corresponding to the fundamental OH-stretching region (3100-4900 cm^{-1}) from Spectrasil and Suprasil-2 samples, both containing $\sim 10^3$ ppm OH are shown in Fig. 1. The absorbance scale was expanded to show the presence of weak, newly observed components. Components previously reported at 3690, 3665, 3605-3620, and 3510 cm^{-1}[2] occur within the saturated peak. Fig. 1 shows a pronounced shoulder at 3850 cm^{-1} and a weak maximum at 4520 cm^{-1}. The weak foot at 4100 cm^{-1} and the shoulder near 4450 cm^{-1} constitute newly observed features.

The 3100-4900 cm^{-1} region of the spectrum is also shown in Fig. 2 for a deuterated sample of Spectrasil. The appearance of a resolved maximum at 3340 cm^{-1} is noteworthy.

To show the OD-stretching region of the deuterated sample without interference from silica overtones, an FTIR difference spectrum, $A_{OD} - k\,A_{OH}$ (here k=3.981) computed from a linear combination of deuterated, A_{OD}, and undeuterated, A_{OH}, absorbance spectra, was required, Fig. 3. The OD-stretching shoulder shown in the figure near 2850 cm^{-1} is the analog of the OH-stretching shoulder at 3850 cm^{-1}.

Infrared difference peaks at 775 ± 10 and 950 ± 10 cm^{-1} were obtained from Suprasil-2 and deuterated TO-8, Fig. 4. The peak at 950 ± 10 cm^{-1} was observed and assigned in previous Raman studies[5,6,11] to Si versus OH stretching. The peak at 775 ± 10 cm^{-1} is new, and is assigned to the torsional oscillation γ(OH) of protons in bent Si-O-H units.

The major components of the fundamental OD-stretching contour were also obtained from infrared difference spectra, $A_{OD} - k\,A_{OH}$. Computer analysis revealed four Gaussian components near 2720 ± 10, 2700 ± 10, 2670 ± 10, and 2595 ± 20 cm^{-1}.

All results of this section are tabulated in Table I.

B. First, Second, and Third Overtone OH-Stretching Contours of Pure Silica

Infrared absorbance spectra corresponding to the first, second, and third OH-stretching overtones have been obtained using optical fibers. These spectra are shown in Figs. 5, 6, and 7. Each of the contours was analyzed into Gaussian components as shown in the figures. It is evident that the decomposition could be accomplished with four components, and that the set of components is very similar for each overtone, both in relative amplitude and in relative width.

The Gaussian component peak frequencies $\bar{\nu}$ from Figs. 5, 6, and 7 are plotted in terms of $\bar{\nu}/v$ versus v in Fig. 8. (The vibrational quantum number of the upper state is here designated by v.) When the apparently related components of the various overtones are connected by smooth lines, correlation with the fundamental is obvious and unequivocal. (Anharmonicity requires that the curves decrease monotonically.) The curved lines shown in Fig. 8 represent least squares fits to an equation in which $\bar{\nu}/v$ is quadratic in v. The curves labeled 1, 2, and 3 have similar shapes (downward concavity), whereas the curve labeled A, has a markedly different shape (upward concavity). An explanation for the opposite curvature of curve A involving a combination vibration is given in Section 4(B).

Components corresponding to the fundamental region and to the Gaussian components of Figs. 5, 6, and 7 are bracketed in Table I, and grouped according to the correlations of Fig. 8 in Table II.

C. Raman Spectrum of the First OH-Stretching Overtone

Raman spectra of the OH-stretching overtone were obtained using pure fused silica optical fibers with OH contents between 500 and 1300 ppm. The Raman signal obtained was 10^4 times weaker than the fundamental signal, in part because of decreasing system sensitivity at the Raman wavelength. Broad weak asymmetric contours on a strongly sloping background were observed which peaked near 7225 ± 50 cm^{-1}. The Raman overtone contour exhibited rapid high-frequency fall-off and a low-frequency tail, *i.e.*, its appearance was similar to that of

the fundamental. The agreement between the overtone Raman peak position at 7225 ± 50 cm^{-1} and the first infrared overtone at 7260 cm^{-1} is satisfactory in view of the weakness of the Raman spectra.

D. First and Second OH-Stretching Overtone Absorptions from GeO_2-doped Optical Fibers

We also obtained OH-stretching overtone spectra of GeO_2-doped optical fibers. Both the graded-index multimode fibers, and the step-index single mode fibers, described earlier, were employed. For the graded-index fiber, a length of 500 m was needed to obtain the first overtone spectrum, and a length of 900 m was required for the second overtone. The third overtone could not be observed clearly because of the low OH content (<1 pmm). Also the Rayleigh scattering loss is predominant over the OH absorption loss at the shorter wavelengths resulting in a very steep background level above which the absorption profile had to be measured. These spectra are shown in Figs. 9 and 10. As in the case of the spectra from pure silica fibers, we could resolve each OH-stretching contour into four Gaussian components, two broad and two narrow, with similar relative heights and widths for the three overtones. However, when Figs. 5 and 6 are compared to Figs. 9 and 10, it is apparent that a major difference results from the GeO_2 doping, namely, that the amplitude and breadth of component 2 increased for the doped sample. Instead of being slightly weaker and slightly broader than component 1, as for pure silica, component 2 becomes much more intense and much broader, resulting in a significant broadening of the entire OH-stretching contour.

Finally, an example of intermediate GeO_2 doping is shown in Fig. 11. Here the spectrum corresponds to the first OH-stretching overtone from a single mode fiber, with a GeO_2 concentration of 4-5 percent. This contour was also decomposed into four Gaussian components, with component 2 displaying a relative width (but not a relative amplitude) intermediate between that from the pure silica and the graded-index fibers.

The relative peak heights and half-widths of the Gaussian components from the pure silica and GeO_2-doped silica are given for the fundamental and overtone vibrations in

Table II.

4. Discussion and Assignments

A. The Fundamental OH Spectrum

Components observed in the fundamental OH-stretching spectrum are listed in Table I. The components at 3510, 3605-3620, 3665, and 3690 cm^{-1} have been previously identified with OH-stretching vibrations involving different silica environments.(2) Their analogs in the OD spectrum are also listed in Table I. The set of neighboring OH components at 3850, 4100, and 4450-4520 cm^{-1}, however, cannot refer to fundamental OH-stretching vibrations, because the fundamental OH-stretching frequency from H_2O extrapolated to zero density at 400 C is 3750 cm^{-1}.(12) Thus, it appears that these components are combinations with silica vibrations.

For fused silica, strong infrared absorption peaks occur near 1110, 810, and 450 ± 10 cm^{-1} (this work). Further, Raman features within the one-phonon region occur near 60 (peak), 115 (shoulder), 280 (shoulder), 350-375 (shoulder), 432 (peak), 490 (peak), 605 (peak), 800 (peak), 825 (shoulder), and 1060 (peak) cm^{-1}.(6,13) The 1060-1110 cm^{-1} vibration arises from Si-O stretching,(6) the 800-810 cm^{-1} vibration from Si-O-Si bending,(14) and the 432-450 cm^{-1} vibration may arise from an oxygen vibration along the Si-O-Si bridging bisector in which no Si motion is involved.(15) The 490 and 605 cm^{-1} peaks arise from silica network defects.(6,13) The remaining frequencies are poorly understood.

Although a complete vibrational picture is lacking, it is expedient in this work to employ a grossly over-simplified nomenclature. This nomenclature happens to employ four vibrations which are convenient for our further analysis, and which refer to the T_d symmetry that the SiO_4 tetrahedra would have if they were not linked on all corners to neighboring tetrahedra, namely, $\bar{\nu}_3 = 1060(1110)cm^{-1}$, $\bar{\nu}_1 = 800(810)cm^{-1}$, $\bar{\nu}_4 = 432(450)cm^{-1}$, and $\bar{\nu}_2 \approx 280\ cm^{-1}$.(16) (Recent Gaussian component analysis of Raman contours has indicated that $\bar{\nu}_2$ may be closer to 240 cm^{-1} or below.(17)) Further, to distinguish silica from OH

vibrations, we append the suffixes SiO_2 and OH to the vibrational designations.

Using the nomenclature described, we assign the four features between 3850 and 4520 cm^{-1} as follows: 3850 cm^{-1}, $\bar{\nu}_3(OH) + \bar{\nu}_2(SiO_2)$; 4100 cm^{-1}, $\bar{\nu}_1(OH) + \bar{\nu}_4(SiO_2)$; 4450 cm^{-1}, $\bar{\nu}_1(OH) + \bar{\nu}_1(SiO_2)$; and 4520 cm^{-1}, (possibly) $\bar{\nu}_4(OH) + \bar{\nu}_3(SiO_2)$. Evidence for these assignments is presented in Section B.

B. Overtone Spectra

From the assignments of the fundamental OH vibrational spectrum given in Section A, it is possible to treat the overtone spectra in a satisfactory manner, consistent with anharmonicity and infrared overtone activity. In Fig. 8, Section 3(B), we identified the $\bar{\nu}/v$ values for $v = 1$ on curves 1, 2, and 3 as OH-stretching fundamental components. In Section 4(A) we assigned the A curve of Fig. 8 to a combination tone. However, treatment of the 3850 cm^{-1} combination by the method of Fig. 8 yields a curvature different from that of components 1, 2, and 3. The combination labeled A in Fig. 8 refers to the case where

$$\frac{\bar{\nu}}{v} = \frac{\bar{\nu}(OH)}{v} + \frac{\bar{\nu}(SiO_2)}{v} \quad . \tag{4}$$

Here, $\bar{\nu}(OH)$ refers both to fundamental and overtones, whereas $\bar{\nu}(SiO_2)$ refers only to the fundamental, and v refers only to the OH vibrational levels. Because $\bar{\nu}(SiO_2)$ is constant, $\bar{\nu}(SiO_2)/v$ decreases with increasing v, and thus the curvature of component A, Fig. 8, must be different from the curvatures of components 1, 2, and 3. (The treatment of combinations according to eqn. (4) reduces the number of phonons in the combination to a minimum for the various OH overtones.)

Component A and other combination tones are better treated by the method of Fig. 12. In Fig. 12 the quantity $[\bar{\nu} - \bar{\nu}(SiO_2)]/v$ is plotted versus v. Here $\bar{\nu}$ refers to combination vibrations. The case where $\bar{\nu}(SiO_2) = 0$ yields curves 1, 2, and 3, taken from Fig. 8. Definitions of other quantities, eqn. (4), still apply.

Consider next the three frequencies of Table I at 4450, 8065, and 11470 cm^{-1}, which are assigned as $\bar{\nu}_1(OH) + \bar{\nu}_1(SiO_2)$, $2\bar{\nu}_1(OH) + \bar{\nu}_1(SiO_2)$, and $3\bar{\nu}_1(OH) + \bar{\nu}_1(SiO_2)$, respectively. From Fig. 12, it is evident that these combinations fit reasonably well to curve 1, for the case where $\bar{\nu}_1(SiO_2) = 800\ cm^{-1}$.

Now consider the four frequencies of Table I at 3850, 7380, 10750, and 13950 cm^{-1}. Again from Fig. 12, it is evident that these four frequencies fit curve 3 reasonably well for $\bar{\nu}_2(SiO_2) = 280\ cm^{-1}$, or even better for the Gaussian component value of 240 cm^{-1}.[17] The assignments are as follows: 3850 cm^{-1}, $\bar{\nu}_3(OH) + \bar{\nu}_2(SiO_2)$; 7380 cm^{-1}, $2\bar{\nu}_3(OH) + \bar{\nu}_2(SiO_2)$; 10750 cm^{-1}, $3\bar{\nu}_3(OH) + \bar{\nu}_2(SiO_2)$; and, 13950 cm^{-1}, $4\bar{\nu}_3(OH) + \bar{\nu}_2(SiO_2)$.

Finally, the frequencies of 4100, 4520, and 7920 cm^{-1} are assigned in Table I to the combinations, $\bar{\nu}_1(OH) + \bar{\nu}_4(SiO_2)$, $\bar{\nu}_4(OH) + \bar{\nu}_3(SiO_2)$, and $2\bar{\nu}_3(OH) + \bar{\nu}_1(SiO_2)$, respectively. Again from Fig. 12, it is evident that reasonable fits are obtained for $\bar{\nu}_4$, $\bar{\nu}_3$, and $\bar{\nu}_1(SiO_2)$ values of 432, 1060, and 800 cm^{-1}, respectively.

One problem would appear to arise from the above combination assignments involving the 280 and 800 cm^{-1} vibrations, in that neither of these vibrations corresponds to the highest infrared intensity. However, computer analysis of infrared absorbance spectra, indicates that the integrated absorbance of the 280 cm^{-1} Gaussian component may be roughly 30-50 percent of the integrated absorbance at 450 cm^{-1}. Further, Gaussian computer analysis of Raman contours from fused silica indicates that the 280 cm^{-1} component (closer to 240 cm^{-1}) is one of the strongest components in the spectrum.[17] The 800 cm^{-1} feature, of course, is prominent in both the Raman and infrared spectra. Thus, the intensity problem, if it exists, does not seem compelling compared to the treatment of Fig. 12, which appears to require vibrations at 280 and 800 cm^{-1}.

C. Comparisons Involving Overtone Components from GeO_2-doped Fused Silica

Comparisons of Gaussian OH-stretching overtone components between Figs. 5 and 6 and Figs. 9 and 10 indicate that the most conspicuous difference involves component 2. The

amplitude and width of this component increases with GeO_2 doping compared to the other components, especially component 1.

In wet fused silica, component 1 is thought to refer to OH oscillators that are essentially gas-like, whereas component 2 is thought to refer to strongly bent O—H···O units, hence nonhydrogen-bonded.[2] The intensification of component 2, relative to component 1 in GeO_2-doped fused silica, suggests that the presence of GeO_2 removes those environments, *e.g.*, gas-like or dangling OH groups whose presence gives rise to the high-frequency OH component, 1. Further, the broadening of component 2 indicates a more varied environment for the doped glass, compared to pure fused silica.

In regard to a more varied environment in GeO_2-doped fused silica, it should be stated that Raman spectra from fused silica doped with 13 percent GeO_2 show features not present in either pure fused silica or pure GeO_2 glass, namely, weak components at 675 and 1000 cm^{-1}.[18] These new features are probably associated with Ge-O-Si bridges. Such bridges would lead to a more varied environment in the mixed glass, and Ge-O-Si-OH as well as Si-O-Ge-OH linkages would be expected to occur.

Finally, the fundamental OH-stretching Raman peak from wet GeO_2 glass occurs near 3590-3600 cm^{-1} and a prominent low-frequency shoulder is also present.[5] These Raman OH-stretching features from wet GeO_2 glass would correspond to components 3 and 4 of Table II. However, it is component 2 that shows the strong relative intensification and broadening with GeO_2 addition. Thus, from this observation and from examinations of frequency shifts of various components, it is evident that Figs. 9 and 10 are *not* simple superpositions of spectra from OH in pure silica or pure GeO_2 glass.

5. Summary

The infrared OH-stretching absorption contours from pure and GeO_2-doped fused silica corresponding to the fundamental and first three overtone regions have been examined and analyzed into Gaussian components. The fundamental spectral region has been shown to

consist of several OH-stretching fundamentals due to different silica environments, plus several nearby combinations involving silica vibrations. The fundamental component substructure has been found to carry over into each of the overtones resulting in a consistent pattern in good agreement with the requirements of anharmonicity and infrared activity. Critical assumptions concerning assignments of components in the fundamental region have been verified by comparisons with deuterated samples. The detailed overtone contours were obtained by using silica fibers, both pure and GeO_2-doped, having lengths to 900 m. The major difference between the pure and GeO_2-doped silica overtone contours involves a relative intensification and broadening of one of the Gaussian OH-stretching components, which is related to structural changes in the binary glass network. The resultant OH-stretching overtone contours from GeO_2-doped silica are considerably broader than from pure silica, primarily because of the broadening of this one component.

6. Acknowledgements

Special thanks are due to Dr. G. B. Wilmot, Research Department, Naval Surface Weapons Center, Dehlgren, Virginia 22448, for making the Nicolet 7000 FTIR available for use and for generous assistance with it. The Raman instrument used in this work was purchased through a grant from the National Science Foundation, Chemical Thermodynamics Program, CHE-77-09888. The work was also funded in part by an ONR Contract at Howard University (Laser-Chemistry). We acknowledge the assistance of D. L. Bisbee for drawing some of the silica fibers, and C. A. Burrus for preparing the deuterated samples.

7. Appendix

A. Force Constants and Anharmonicity

The specific groupings of Gaussian OH-stretching components of Table II, and the correlations of Fig. 8, involved considerations of anharmonicity. In Fig. 8, for example, a criterion was employed that all correlations must involve negative slopes, $d(\bar{\nu}/\nu)/d\nu$, as

demanded by anharmonicity. Moreover, anharmonicity, mechanical and/or electrical, must be present for infrared and Raman overtone activity to occur at all. Thus, an infrared component in the fundamental OH-stretching spectrum at 3690 cm^{-1} may not be correlated with an overtone $\bar{\nu}/2$ position of 3690 cm^{-1}, because overtone activity would be forbidden. Instead the 3690 cm^{-1}, fundamental is correctly correlated with an overtone $\bar{\nu}/2$ position of 3630 cm^{-1}, Table II. Additional evidence for the correlations of Fig. 8 and the groupings of Table II comes from more detailed aspects of anharmonicity, Table III.

The fundamental infrared OH-stretching peak occurs near 3665 cm^{-1}, and the fundamental Raman peak near 3690 cm^{-1}.(2) From these values it was decided, Table III, that the first, second, and third overtone peaks correlate with the fundamental Raman peak rather than with the fundamental infrared peak. A factor in this decision involved the first difference, Δ_1, between successive $\bar{\nu}/v$ values. Also peak positions are more accurate than component positions.

Consider that the fundamental and overtone frequencies are given by $\bar{\nu} = av - bv^2$, or $\bar{\nu}/v = a - bv$. This means that first differences in $\bar{\nu}/v$ values between neighboring vibrational levels are constant and equal to $(-b)$. From Table III, it is evident that first differences Δ_1 are much more constant for row 2 where the fundamental Raman peak value is compared, than for row 1, where the fundamental infrared peak is compared. This indicates that the fundamental infrared peak is anomalous, *i.e.*, that the infrared intensity at 3690 cm^{-1} is unexpectedly weak, and it attests to the validity of the Raman and overtone comparisons, *viz.*, that the 3690 cm^{-1} component should be compared with the first, second, and third overtone components at 3630, 3665, and 3480 cm^{-1}, resp., Table II.

The second differences Δ_2 of Table III suggest that a cubic rather than a quadratic equation in v is involved, *i.e.*, $\bar{\nu}/v = a - bv + cv^2$, because they are constant, (+2c, or -10 cm^{-1}). In regard to constancy of Δ_2, the peak data of Table III involving the Raman comparison are plotted in Fig. 8, along with component 1 values, which refer essentially to peak

values. Both plots indicate constant curvature, $d^2(\bar{\nu}/v)/dv^2 = 2c = \Delta_2$, as do the plots for components 2 and 3.

The least squares equations for component A (despite the fact that it is a combination), and for components 1-3, as well as for the peak values, Table III, are as follows:

(A) $\bar{\nu}/v = 4012 \pm 56 - (179.5 \pm 51.1)v + (12.5 \pm 10.1)v^2$,

(1) $\bar{\nu}/v = 3734 \pm 9 - (38.3 \pm 8.5)v + (-6.3 \pm 1.7)v^2$,

(2) $\bar{\nu}/v = 3692 \pm 6 - (15.5 \pm 5.7)v + (-12.5 \pm 1.1)v^2$,

(3) $\bar{\nu}/v = 3624 \pm 45 - (-1.9 \pm 41.5)v + (-16.8 \pm 8.2)v^2$,

and (peak) $\bar{\nu}/v = 3740 \pm 1.7\times10^{-4} - (45.0 \pm 1.6\times10^{-4})v + (-5.0 \pm 3.1\times10^{-5})v^2$.

The positive curvature for component A, $\frac{d^2(\bar{\nu}/v)/dv^2}{2} = +12.5 \pm 10.1$, compared to the negative curvature value of $-(6.3 \pm 1.7)$, $-(12.5 \pm 1.1)$, $-(16.8 \pm 8.2)$, and $-(5.0 \pm 3.1\times10^{-5})$, respectively, for components 1-3 and the peak agree with the differing assignments, namely combinations versus overtones, Table I. Further, the b values *must* be positive, but the c values can be *either positive or negative*. *All b values are positive, except* for component 3 which yields $b = (-1.9 \pm 41.5)$. This b value is uncertain because of errors in component 3 peak frequency, and thus the negative sign is probably not significant.

The coefficients in the cubic equations $\bar{\nu} = av - bv^2 + cv^3$ are related to fundamental constants, in cm^{-1}, as follows:

$$a = \omega_e, \quad b = \omega_e x_e, \quad c = \omega_e y_e, \text{ and } \omega_e = a + b + 3/4c. \tag{19}$$

The force constant $k_e = 4\pi^2\mu c^2\omega_e^2$ represents the curvature of the potential, d^2V/dr^2, at the equilibrium position, r_e. Values or ω_e and k_e corresponding to the peak and component frequencies, 1-3, are as follows: (peak), $\omega_e = 3781\ cm^{-1}$, $k_e = 7.99\times10^5\ dyn-cm^{-1}$; (1) $\omega_e =$

3768 cm^{-1}, $k_e = 7.93 \times 10^5$ dyn–cm^{-1}; (2) $\omega_e = 3698$ cm^{-1}, $k_e = 7.64 \times 10^5$ dyn–cm^{-1}; and (3) $\omega_e = 3617$ cm^{-1}, $k_e = 7.31 \times 10^5$ dyn–cm^{-1}.

B. Justification for the Use of Gaussian Components

Because Gaussian components were employed extensively for fundamental and overtone OH-stretching contours in this work, it is desirable to describe various consideration leading to their use. In fused silica, OH oscillators are thought to exhibit several preferred structures, *e.g.*, free or gas-like OH groups (dangling OH groups), strongly bent and thus weak O–H···O hydrogen bonds, and strong or more linear hydrogen bonds.[2] These preferred local structures cause a clustering of the OH frequencies about certains values, namely, the component centers.

The decoupled OH oscillators also sense structural distortions, which are both angular and extensional, and this effect leads to a large broadening about the component centers. Also, because fused silica is amorphous, the structural distortions are essentially random, and hence the component shape is Gaussian. No large Lorentzian character is obvious experimentally, although the Gaussian component shape could be envisioned as the envelope of a very great number of sharp overlapping Lorentzians whose wings are lost in the noise level near the base of the OH-stretching contour.

With regard to preferred local structures, it is useful to give an example which refers to the fundamental OH-stretching component at 3690 cm^{-1}. The 3690 cm^{-1} component occurs at a frequency only 60 cm^{-1} below the zero-density vibrational extrapolation for H_2O gas at 400°C.[12] This indicates that the OH oscillators involved are nearly free or gas-like. A reasonable explanation for this high OH-stretching frequency in fused silica is that adjacent silanol groups are thought to be present, Si-OH HO-Si,[6] and if one OH group engages in a moderately strong and thus nearly linear hydrogen bond, O–H···O, the adjacent OH group must be nearly free or dangling, because of the requirement that the Si–O–H angle is much less than 180°.[20] The situation is shown schematically by

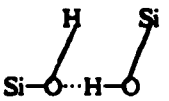

Finally, Gaussian decomposition of Raman contours from pure fused silica in the region between 0 and 1100 cm^{-1} has recently been very successful.[17] Accurate contour fits were obtained using only those Gaussian components whose centers correspond to experimentally observed features, such as peaks and well-characterized shoulders, that is, no extra components were employed.

REFERENCES

1. D. B. Keck, R. D. Maurer, and P. C. Schultz, Appl. Phys. Lett. *22*, 307 (1973).
2. G. E. Walrafen and S. R. Samanta, J. Chem. Phys. *69*, 493 (1978).
3. G. E. Walrafen, S. R. Samanta, and P. N. Krishnan, J. Chem. Phys. *72*, 113 (1980).
4. G. E. Walrafen and S. R. Samanta, J. Chem. Phys. *68*, 4672 (1978).
5. F. L. Galeener and R. H. Geils, "The Polarized Raman Spectra of OH in Vitreous SiO_2 and GeO_2," Symp. Struct. Noncryst. Mater., Cambridge, England, September 23, 1976.
6. R. H. Stolen and G. E. Walrafen, J. Chem. Phys. *64*, 2623 (1976).
7. G. E. Walrafen, Spex Speaker *20*, 1 (1975).
8. G. E. Walrafen, J. Chem. Phys. *62*, 297 (1975).
9. R. W. Lee, R. C. Frank, and D. E. Swets, J. Chem. Phys. *36*, 1062 (1962); A. Farkas and L. Farkas, Trans. Faraday Soc. *31*, 821 (1935).
10. "Optical Fiber Telecommunications," eds. S. E. Miller and A. G. Chynoweth, Acad. Press, New York, 1979.
11. C. M. Hartwig and L. A. Rahn, J. Chem. Phys. 67, 4260(1977).
12. E. U. Franck and H. A. Lindner, dissertation of the latter, Univ. of Karlsruhe, 1970.
13. G. E. Walrafen, P. N. Krishnan, and S. W. Freiman, J. Appl. Phys. *52*, 2832 (1981). G. E. Walrafen and P. N. Krishnan, J. Chem. Phys. *74*, 5328 (1981).
14. R. H. Stolen, J. T. Krause, and C. R. Kurkjian, Discuss. Faraday Soc. *50*, 103 (1970).
15. F. L. Galeener and J. C. Mikkelsen, Jr. Phys. Rev. B, *23*, 5527 (1981).
16. R. V. Adams and R. W. Douglas, J. Soc. Glass Tech. *43*, 147T (1959).

17. G. E. Walrafen and P. N. Krishnan, Appl. Optics --, xxxx (1981).

18. G. E. Walrafen and J. Stone, Appl. Spectrosc. *29*, 337 (1975).

19. M. Avram and G. D. Mateescu, "Infrared Spectroscopy," R. E. Krieger Publ. Co., Huntington, New York, 1978.

20. The Si-O-H angle has been reported as 160° for methylsilanol, J. Rouviere, V. Tabacik, and G. Fleury, Spectrochim. Acta *29A*, 229 (1973).

CAPTION

TABLE I

Suggested assignment for vibrational frequencies in cm^{-1} corresponding to overtone and combination vibrations from fused silica containing OH and OD groups. Values in column 1, %D, refer to % deviation where E is the experimental frequency, and A is the assigned value in cm^{-1}. Rows 1-7 refer to OH(OD) fundamentals. For detailed discussion of interactions leading to components $\bar{\nu}_1$(OH) to $\bar{\nu}_4$(OH) see Ref. (2). Components in each bracket refer to A, 1, 2 ,3, and 4, Table II. Rows 28-31 refer to SiO_2 fundamentals.

TABLE I

	$\%D = \left(\frac{A-E}{A}\right) 100$	OH Vibration Frequency (cm^{-1})	OD Vibration Frequency (cm^{-1})	Suggested Assignment
1		775 ± 10		OH Torsion
2		950 ± 10		Si-OH Stretch
3		1595 ± 10		Si-O-H Bend
4		3510 ± 10	2595 ± 20	$\bar{\nu}_4$ (OH), (OD)
5		3605 − 3620	2670 ± 10	$\bar{\nu}_3$ (OH), (OD)
6		3665	2700 ± 10	$\bar{\nu}_2$ (OH), (OD)
7		3690	2720 ± 10	$\bar{\nu}_1$ (OH), (OD)
8	1.1,1.6	3850		$\bar{\nu}_3(OH) + \bar{\nu}_2(SiO_2)$,
			2850	$\bar{\nu}_4(OH) + \bar{\nu}_2(SiO_2)$
9	0.5	4100		$\bar{\nu}_1(OH) + \bar{\nu}_4(SiO_2)$
10	1.6		3340	$\bar{\nu}_4(OD) + \bar{\nu}_1(SiO_2)$
11	0.9	4450		$\bar{\nu}_1(OH) + \bar{\nu}_1(SiO_2)$
12	1.1	4520		$\bar{\nu}_4(OH) + \bar{\nu}_3(SiO_2)$
13	1.7	7100		$2\bar{\nu}_3(OH)$
14	1.5	7220		$2\bar{\nu}_2(OH)$
15	1.6	7260		$2\bar{\nu}_1(OH)$
16	1.7	7380		$2\bar{\nu}_3(OH) + \bar{\nu}_2(SiO_2)$
17	1.3	7920		$2\bar{\nu}_3(OH) + \bar{\nu}_1(SiO_2)$
18	1.4	8065		$2\bar{\nu}_1(OH) + \bar{\nu}_1(SiO_2)$
19	32	10490		$3\bar{\nu}_3(OH)$

TABLE I — (Cont'd)

	$\%D = \left[\frac{A-E}{A}\right] 100$	OH Vibration Frequency (cm^{-1})	OD Vibration Frequency (cm^{-1})	Suggested Assignment
20	3.6	[10600		$3\bar{\nu}_2(OH)$
21	3.3	10700		$3\bar{\nu}_1(OH)$
22	3.4	10750]		$3\bar{\nu}_3(OH) + \bar{\nu}_2(SiO_2)$
23	3.5	11470		$3\bar{\nu}_1(OH) + \bar{\nu}_1(SiO_2)$
24	7.0	[13440		$4\bar{\nu}_3(OH)$
25	6.4	13720		$4\bar{\nu}_2(OH)$
26	5.8	13910		$4\bar{\nu}_1(OH)$
27	5.6	13950]		$4\bar{\nu}_3(OH) + \bar{\nu}_2(SiO_2)$
	SiO_2 Vibration			Designation
28	280			$\bar{\nu}_2(SiO_2)$
29	432			$\bar{\nu}_4(SiO_2)$
30	800			$\bar{\nu}_1(SiO_2)$
31	1060			$\bar{\nu}_3(SiO_2)$

CAPTION

TABLE II

Comparison between Gaussian infrared OH-stretching component frequencies for multi-mode GeO_2-doped fused silica, and for pure fused silica optical fibers. Combinations, row A, in parentheses. Rows 1-4, fundamental and overtones, see Table I. Listed under the frequencies of the Gaussian components are the relative peak heights and half widths in cm^{-1}. Half-widths were omitted for the second overtone due to uncertainties.

TABLE II

	$\Delta\bar{\nu}$ or $\bar{\nu}_1$	UNDOPED			DOPED	
		$\bar{\nu}_2/2$	$\bar{\nu}_3/3$	$\bar{\nu}_4/4$	$\bar{\nu}_3/2$	$\bar{\nu}_3/3$
A	(3850)	(3690)	(3600)	(3490)	(3690)	(3585)
	0.03,250 ± 10	0.17,315	0.26,—	0.27,—	0.18,190	0.14,—
1	3690	3630	3565	3480	3615	3535
	0.53,40 ± 5	1.00,95	1.00,—	1.00,—	0.68,100	0.60,—
2	3665	3610	3535	3430	3570	3505
	0.67,70 ± 5	0.86,170	0.82,—	0.64,—	1.00,230	1.00,—
3	3605-3620	3550	3490	3360	3460	3435
	1.00,125	0.20,370	0.36,—	0.23,—	0.18,275	0.22,—
4	3510 ± 10	—	—	—	—	—
	0.17,180±10	—	—	—	—	—

CAPTION

TABLE III

First and second differences, Δ_1 and Δ_2, for comparisons between infrared and Raman fundamental OH-stretching peak frequencies in cm^{-1}, $\Delta\bar{\nu}$ or $\bar{\nu}_1$, with *the corresponding infrared* overtone peak values $\bar{\nu}_2/2$, $\bar{\nu}_3/3$ and, $\bar{\nu}_4/4$, see Table II, row 1. Note that Δ_2 values are constant, $-10\ cm^{-1}$, for the Raman peak comparison, but not for the infrared comparison.

TABLE III

	$\Delta\bar{\nu}$ or $\bar{\nu}_1(cm^{-1})$	$\bar{\nu}_2/2(cm^{-1})$	$\bar{\nu}_3/3(cm^{-1})$	$\bar{\nu}_4/4(cm^{-1})$
INFRARED	3665	3630	3560	3480
Δ_1		−35	−70	−80
Δ_2		−35	−10	
RAMAN	3690	3630	3560	3480
Δ_1		−60	−70	−80
Δ_2		−10	−10	

CAPTION

Fig. 1.

Fourier transform infrared absorbance spectra obtained from Suprasil-2 (lower) and Spectrasil (upper) both containing 10^3 ppm OH. Arrows *refer to* the positions of broad shoulders and peaks. Sample thickness, lower spectrum, 10 mm; upper spectrum, 1 mm. Scale of upper spectrum expanded.

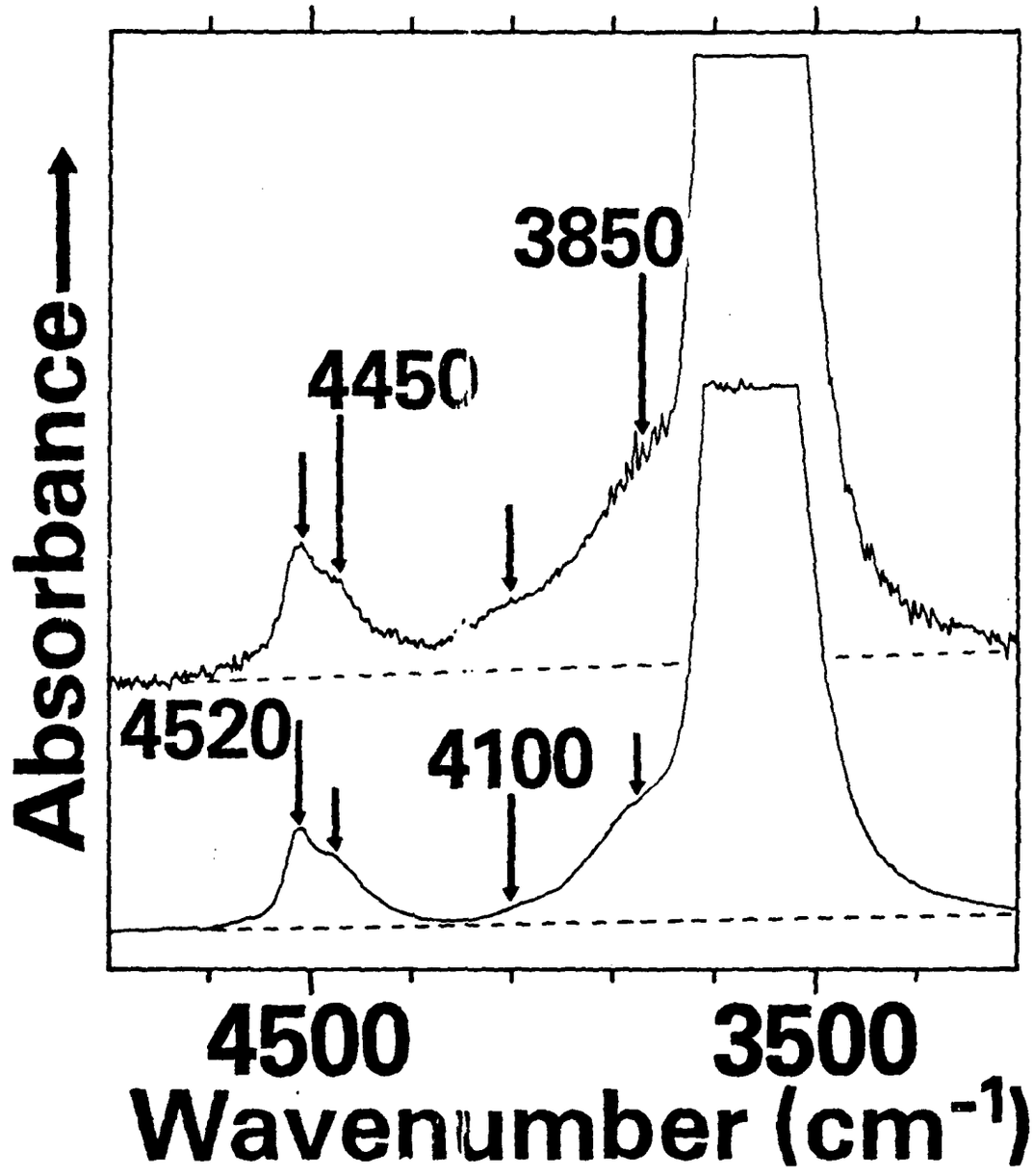
Absorbance
3850
4450
4520
4100
4500
3500
Wavenumber (cm-1)

CAPTION

Fig. 2.

Fourier transform infrared absorbance spectrum from deuterated sample of Spectrasil. Note the fully resolved peak at 3340 cm^{-1} to the right side of the intense saturated maximum. OH-content before deuteration, 10^3 ppm.

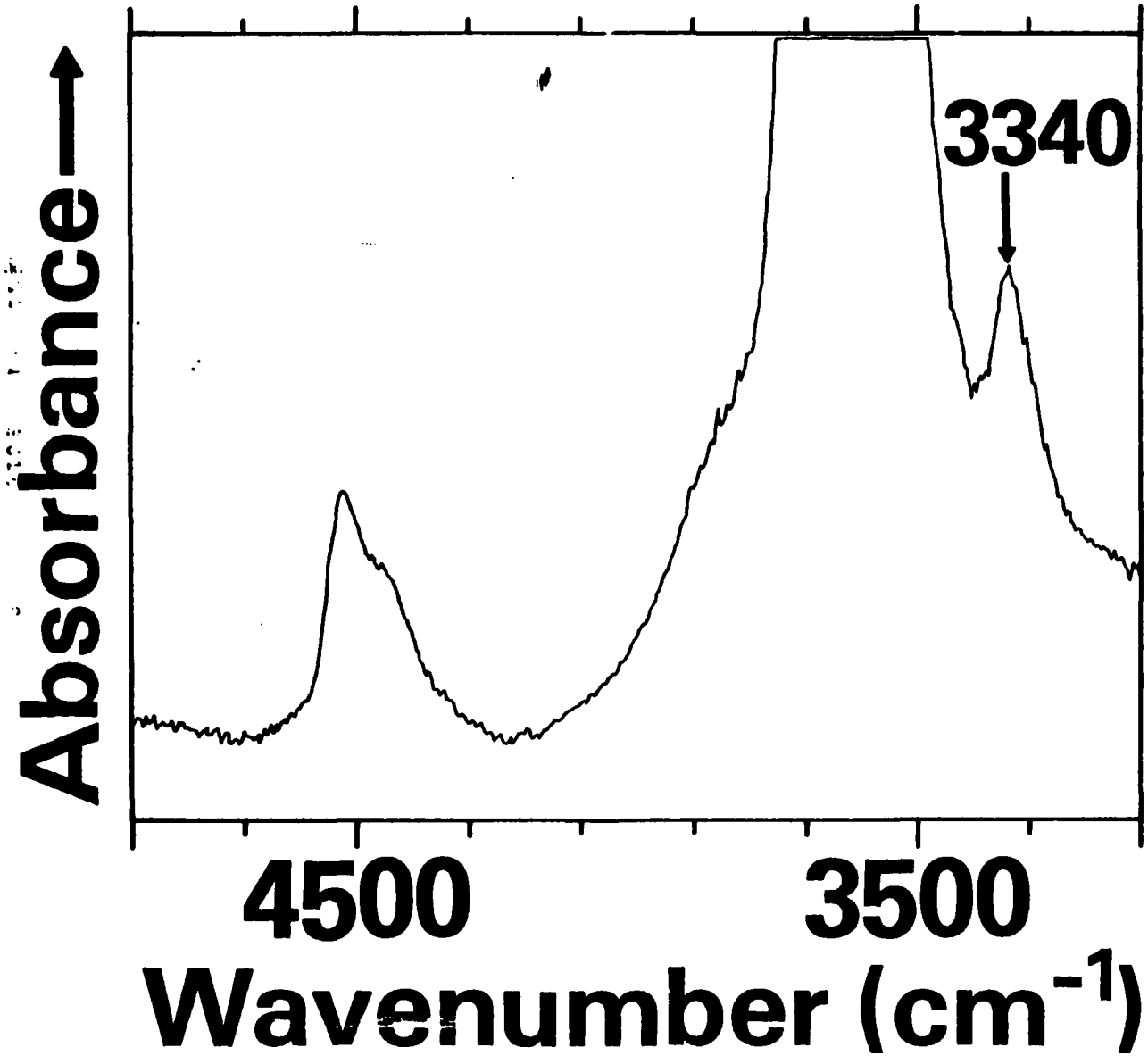
Absorbance
3340
4500
3500
Wavenumber (cm^{-1})

CAPTION

Fig. 3.

Fourier transform infrared difference spectrum obtained from a linear combination of deuterated and undeuterated absorbance spectra. The peak of the intense saturated absorbance shown occurs at 2715 cm^{-1}. The arrow refers to the central position of a broad weak shoulder centered near 2850 cm^{-1}. Overtone vibrations from fused silica which interfered with the OD-stretching peak at 2715 cm^{-1} were removed by the difference method.

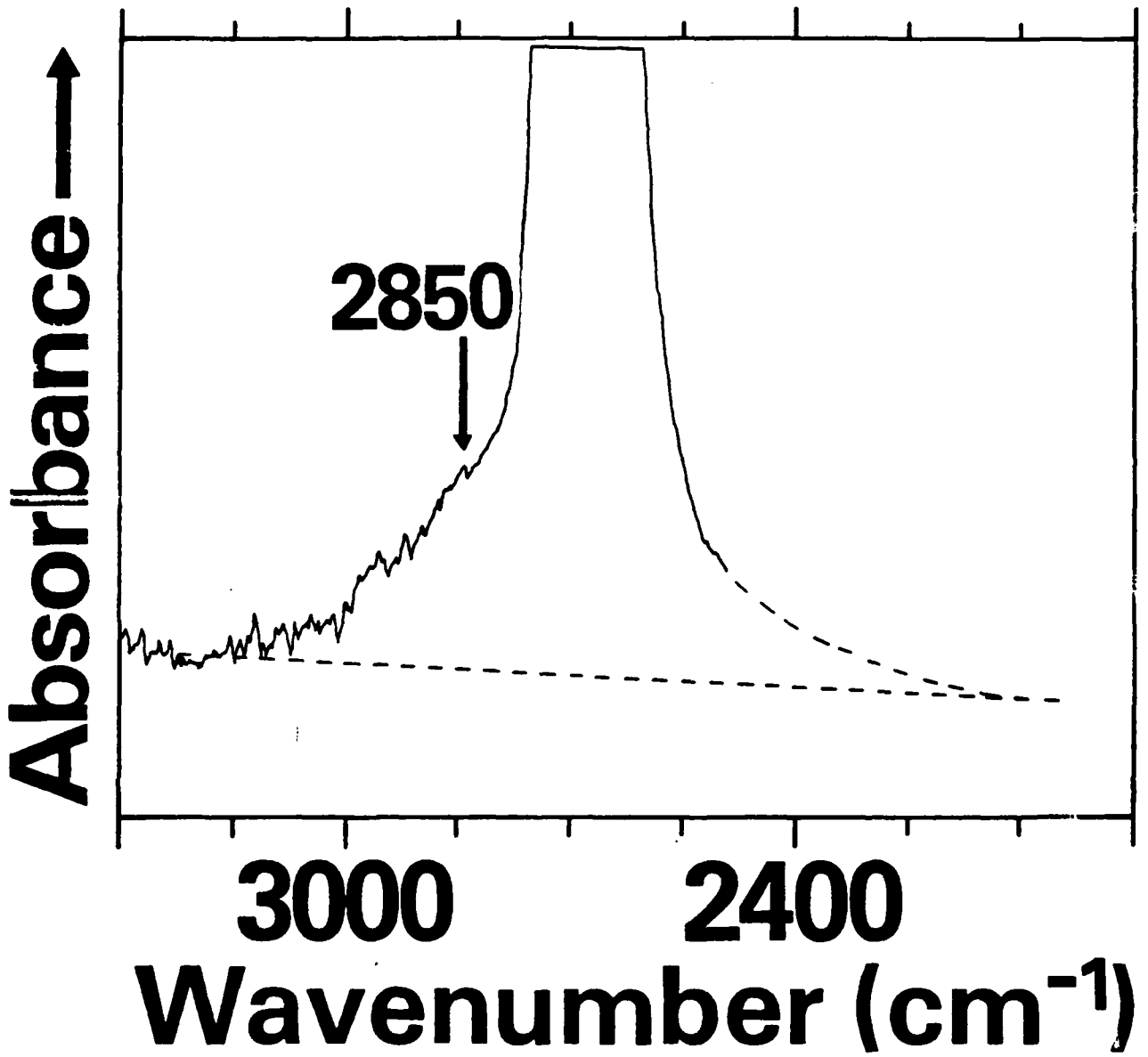
Absorbance
2850
3000
2400
Wavenumber (cm-1)

CAPTION

Fig. 4.

Fourier transform infrared difference spectra obtained from Suprasil-2, 10^3 ppm OH, and deuterated TO-8, OH content before deuteration, 10^2 ppm. Arrows in the upper spectrum emphasize hydrogenic features near 950 and 775 cm^{-1}. The intense peak at 1110 cm^{-1} is a Si—O stretching vibration not fully removed by the difference method. The lower spectra, (a) and (b), refer to the linear combinations $A_{OH} - 1.520A_{OD}$, and $A_{OH} - 1.902A_{OD}$, resp., for 775 cm^{-1} peak, for which the absorbance scale was expanded. The upper spectrum refers to the linear combination $A_{OH} - 1.505A_{OD}$. KBr disk technique.

4 UPPER

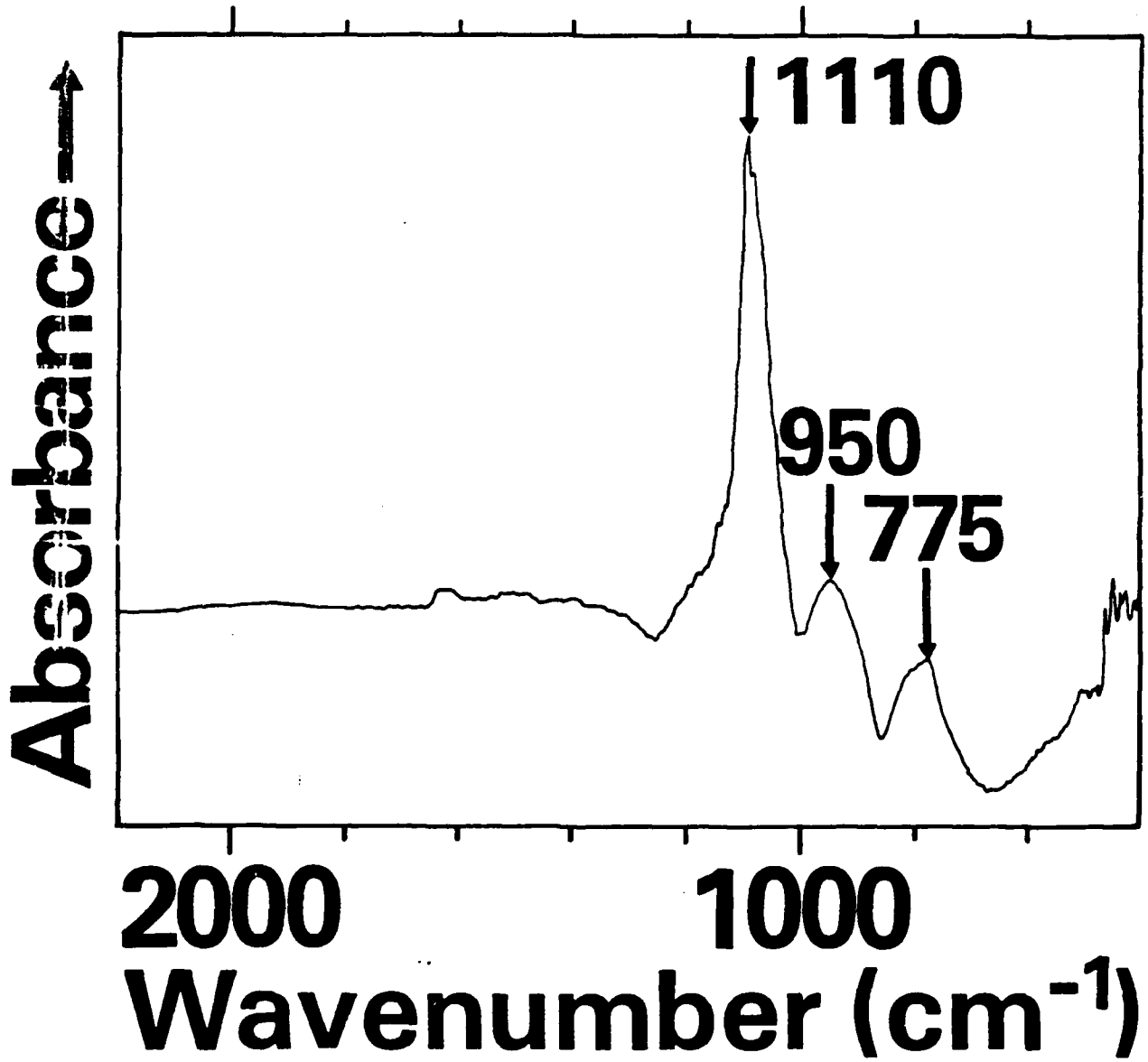

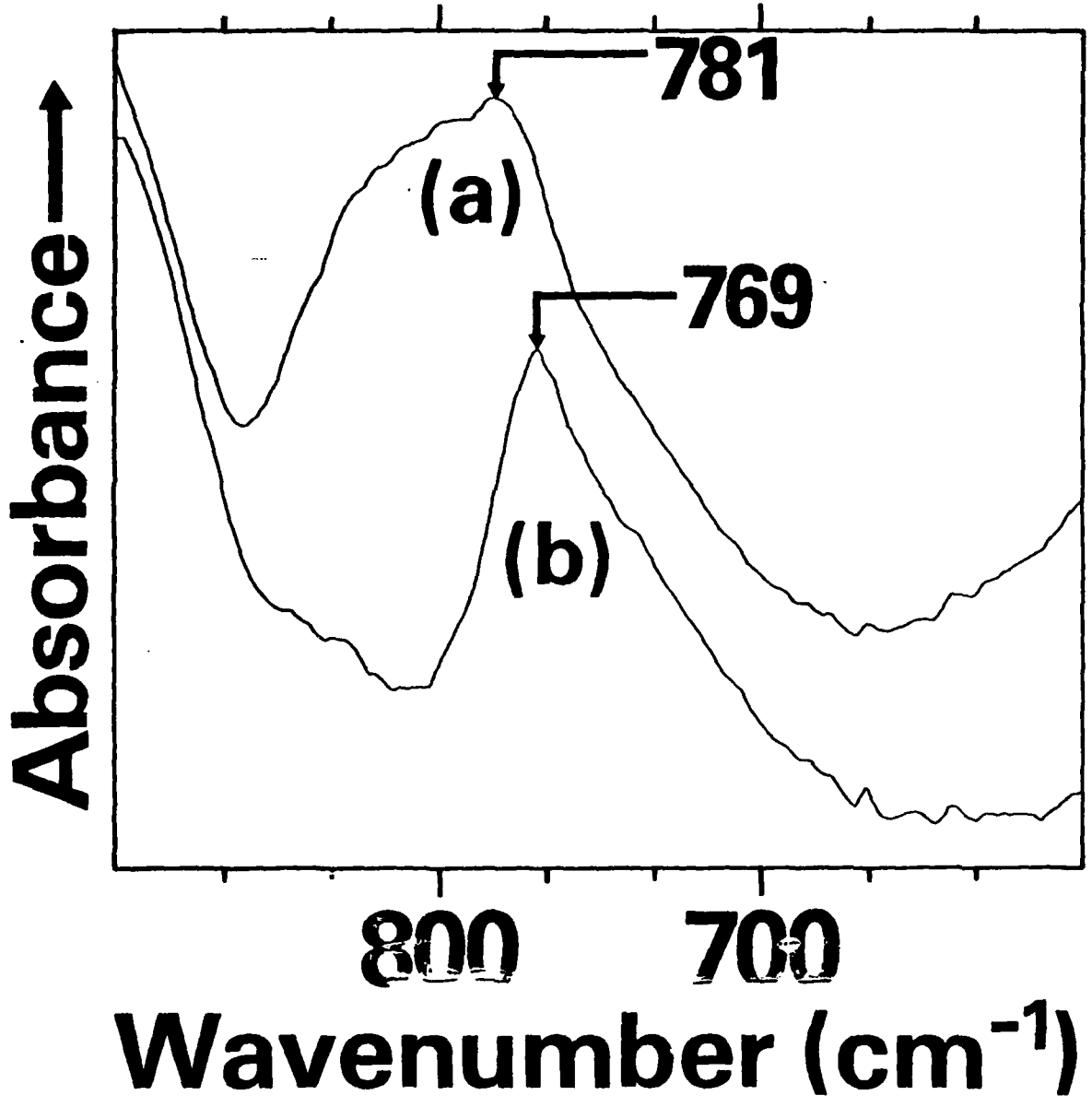

4 LOWER

CAPTION

Fig. 5.

Infrared absorbance spectrum of the first OH-stretching overtone region from pure fused silica optical fiber. Four Gaussian components comprising the contour are shown.

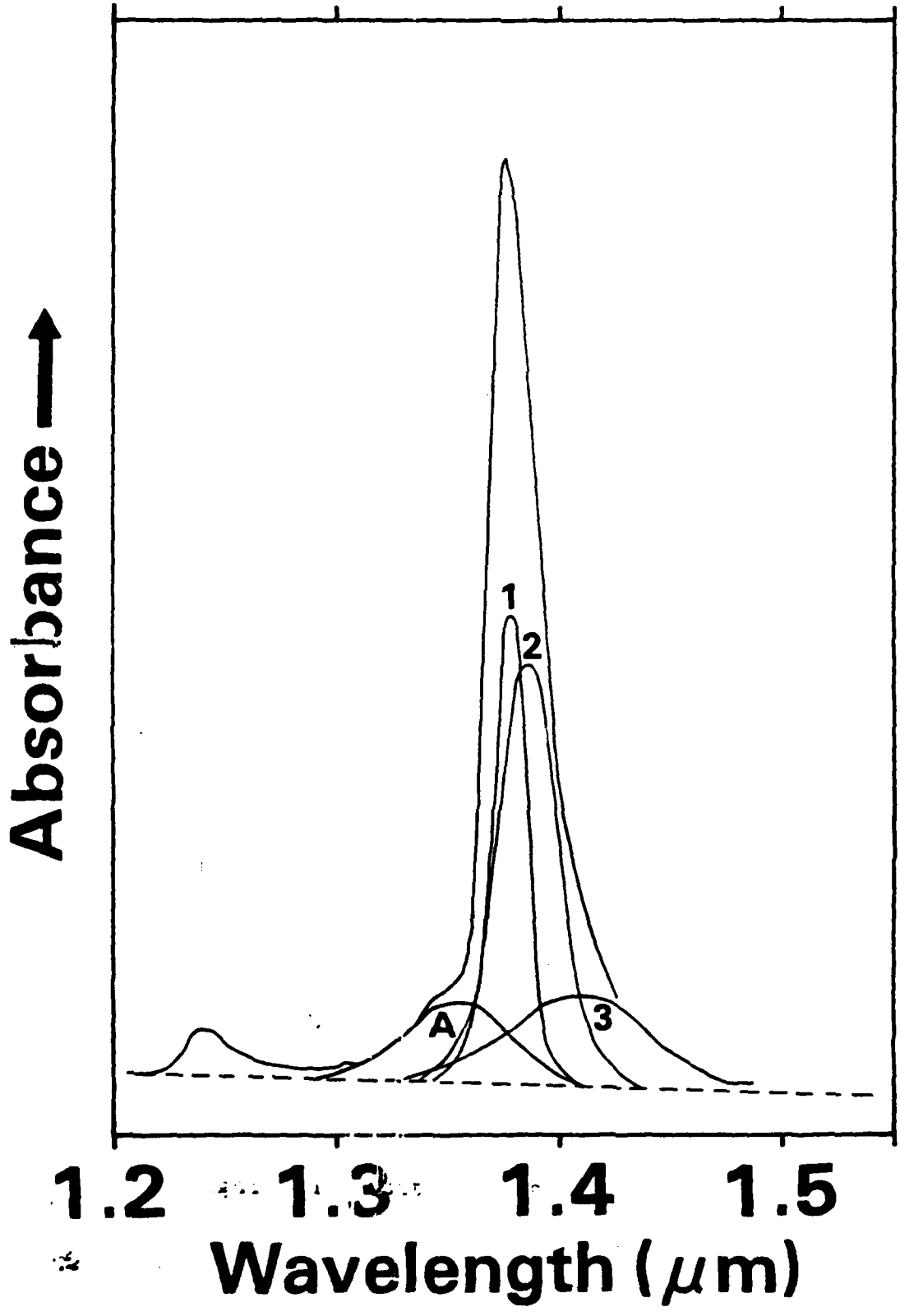
Absorbance
1
2
A
3
1.2
1.3
1.4
1.5
Wavelength (μm)

CAPTION

Fig. 6.

Infrared absorbance spectrum of the second *OH-stretching overtone region* from pure fused silica optical fiber. Four Gaussian components comprising the contour are shown.

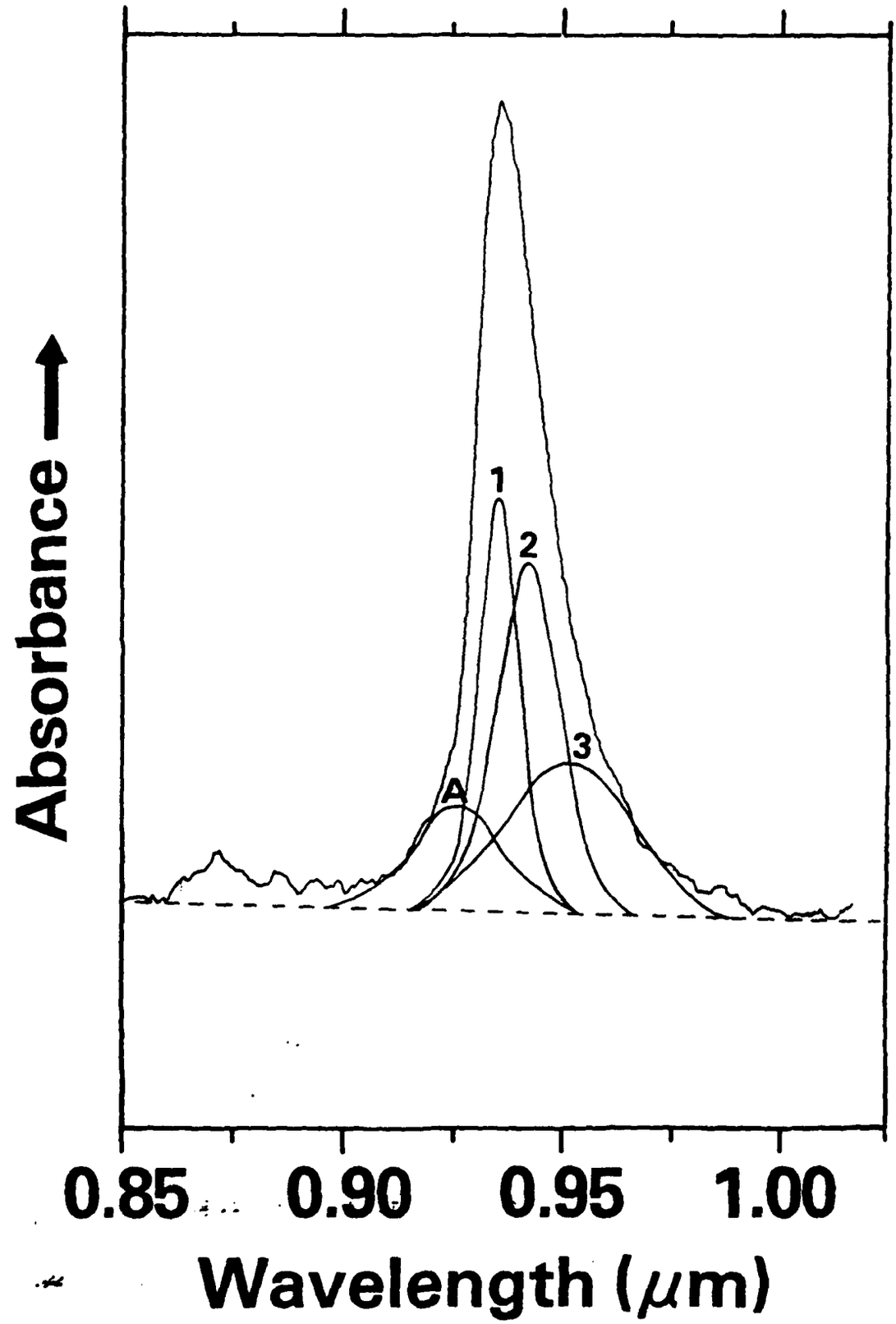
Absorbance
1
2
3
A
0.85
0.90
0.95
1.00
Wavelength (μm)

CAPTION

Fig. 7.

Infrared absorbance spectrum of the third OH-stretching overtone region from a pure fused silica optical fiber. Four Gaussian components comprising the contour are shown.

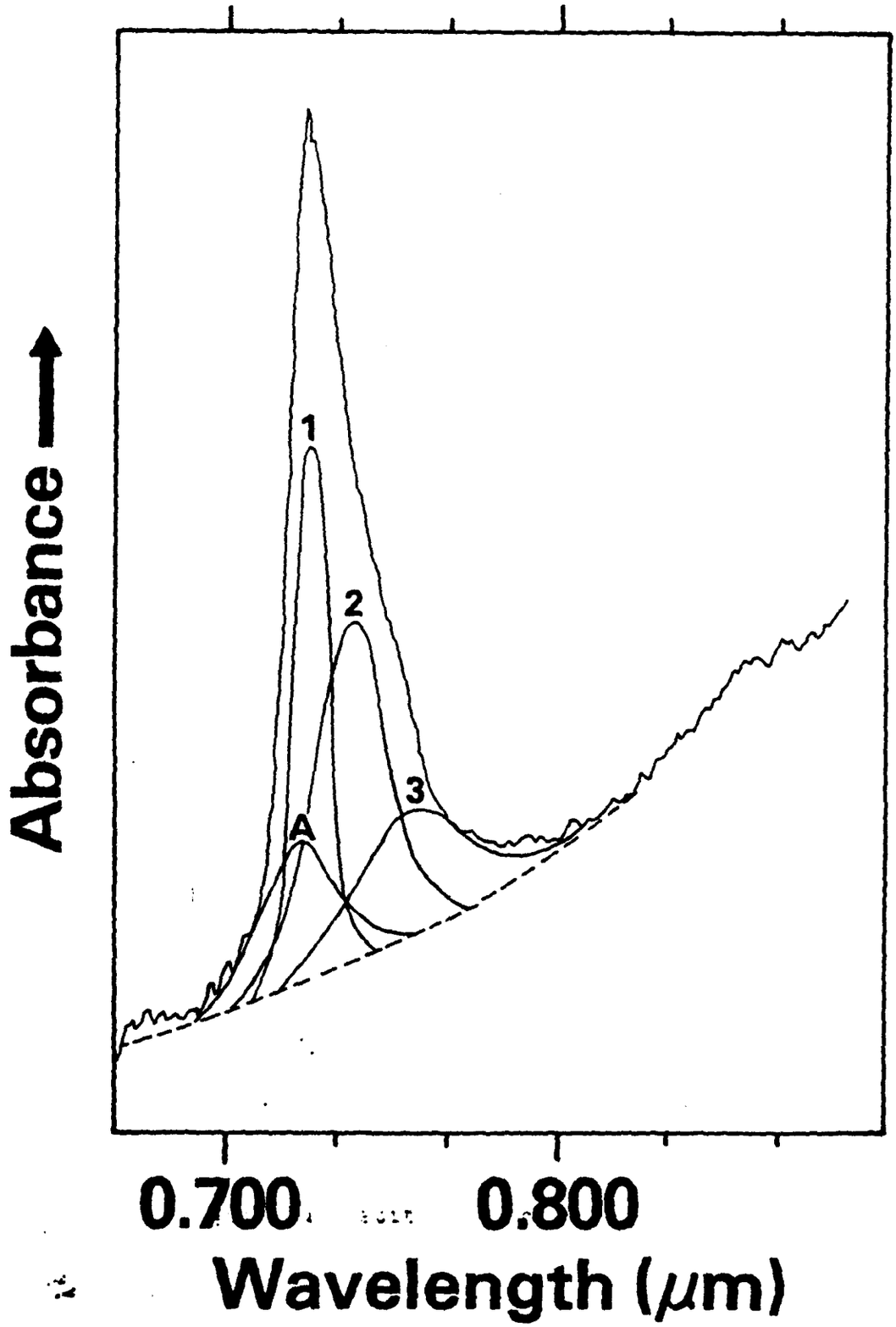
Absorbance
1
2
3
A
0.700
0.800
Wavelength (μm)

CAPTION

Fig. 8.

Plot of $\bar{\nu}/v$ versus v for the peak (diamonds), and Gaussian component centers (circles) of the fundamental, and first, second, and third overtones of the OH-stretching region from pure fused silica. The quantum number of the upper vibrational state is designated by v. Designations of Gaussian components A, 1-4, are the same as those of Table II and Figs. 5, 6 and 7. The intercepts, labeled a_1, a_2, a_3, for curves 1-3, are discussed in the appendix, Section 7(A). Note that the curvature for component A is concave upward, whereas the other components show downward concavity. Component A *refers to a combination vibration*, whereas the other components refer to overtone OH-stretching vibrations.

$\bar{\nu}$/ν, cm^{-1}
4000
3500
a_1
a_2
a_3
A
1
2
3
4
0
1
2
3
4
v

CAPTION

Fig. 9.

Infrared absorbance spectrum of the first OH-stretching overtone region from a GeO_2-doped fused silica optical fiber. Four Gaussian components comprising the contour are shown.

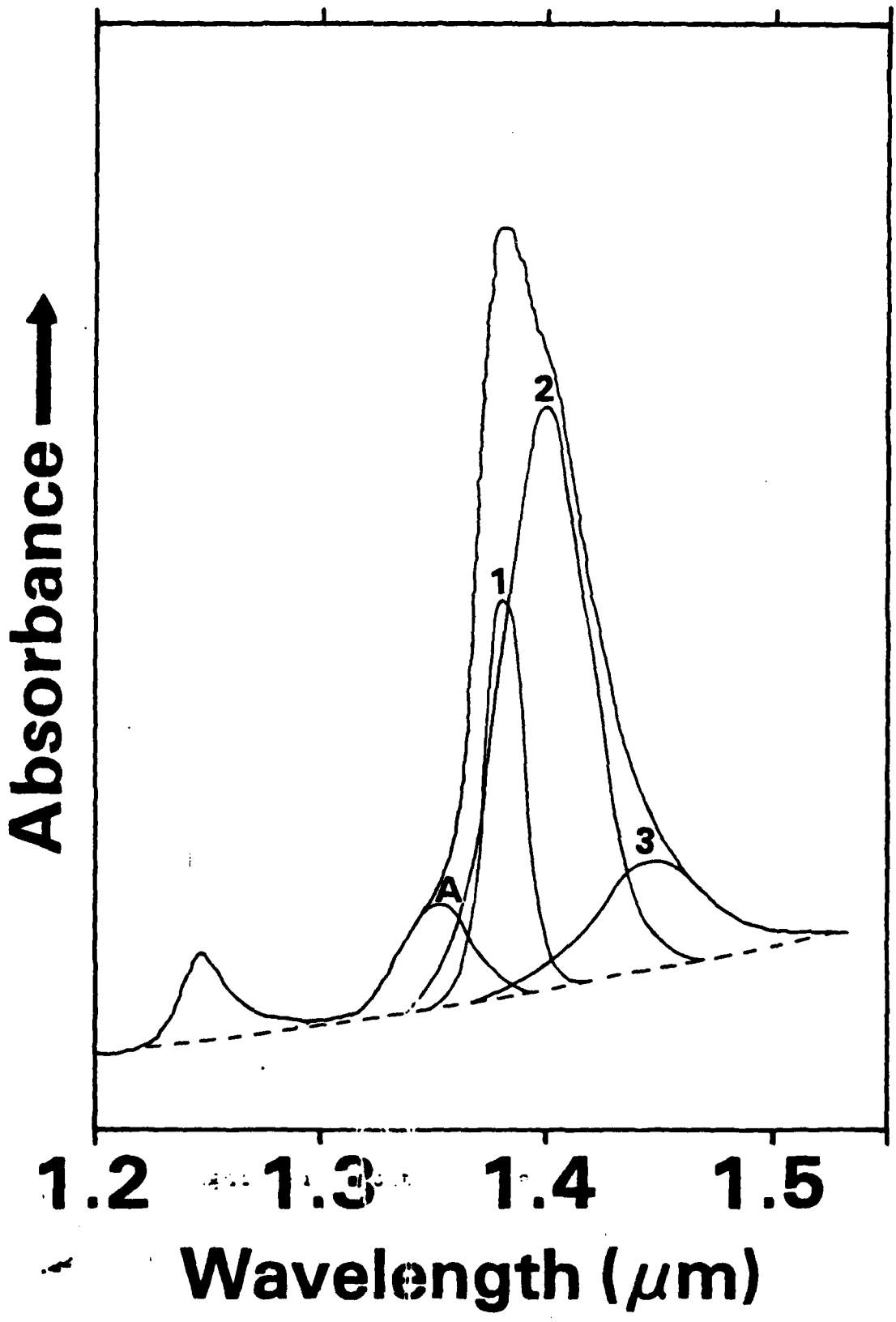
Absorbance
1
2
3
A
1.2
1.3
1.4
1.5
Wavelength (μm)

CAPTION

Fig. 10.

Infrared absorbance spectrum of the second OH-stretching overtone region from GeO_2-doped fused silica optical fiber. Four Gaussian components comprising the contour are shown.

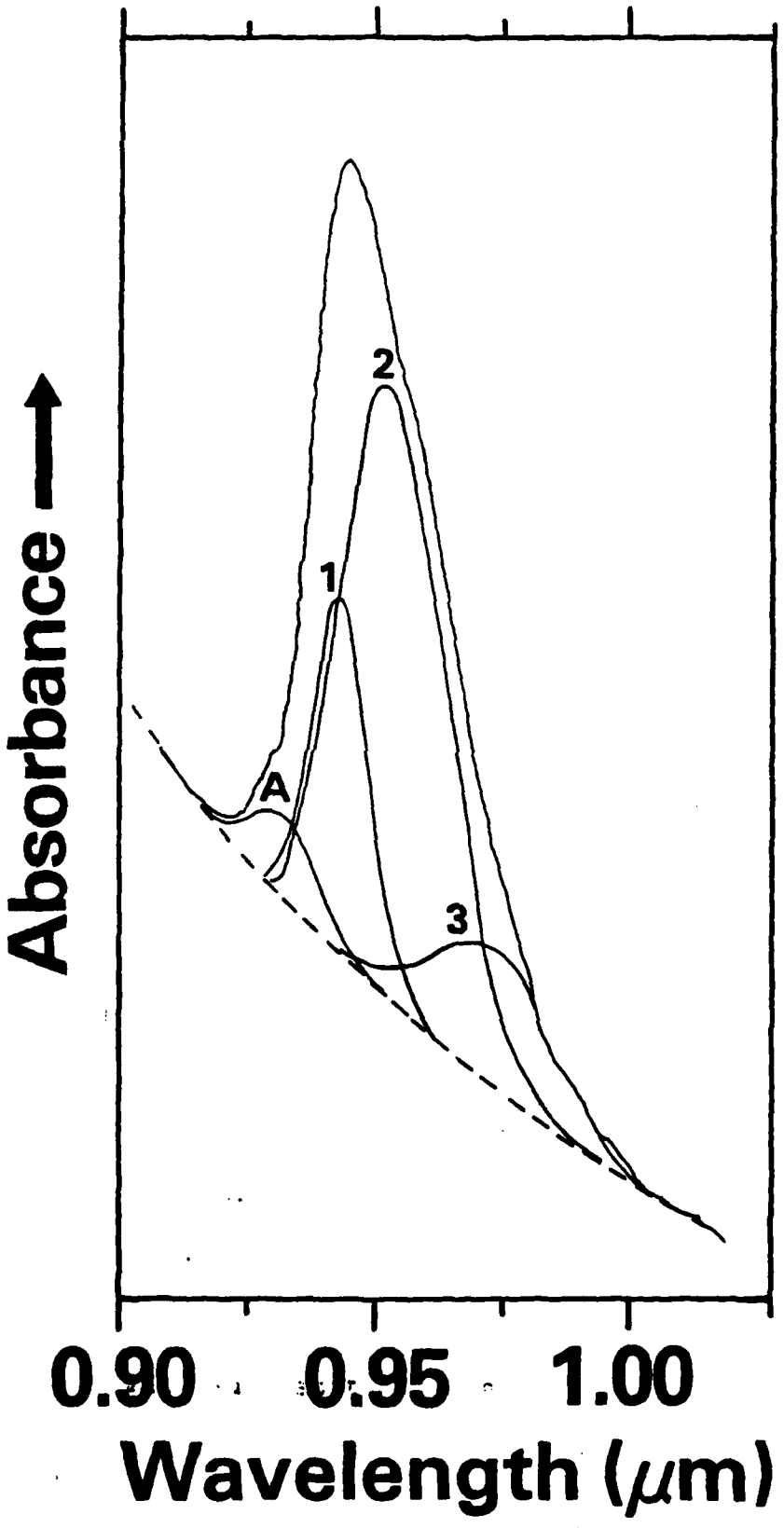
Absorbance
2
1
A
3
0.90
0.95
1.00
Wavelength (μm)

CAPTION

Fig. 11.

Infrared absorbance spectrum of the first OH-stretching overtone region from a *single-mode* GeO_2-doped fused silica optical fiber. (All other fiber spectra in this article refer to multi-mode optical fibers, both GeO_2-doped and pure, fused silica.) Four Gaussian components comprising the contour are shown.

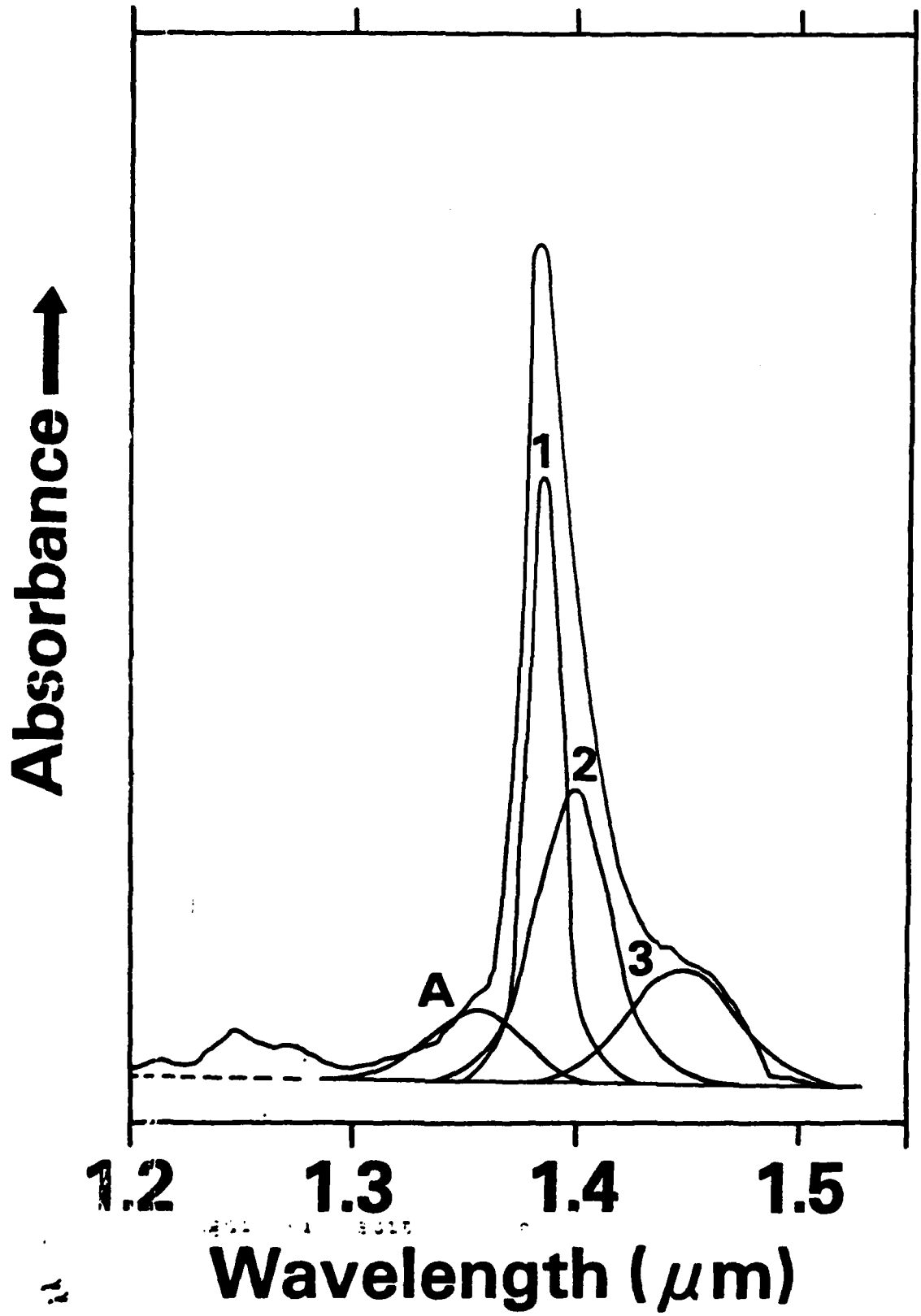
Absorbance
1
2
3
A
1.2
1.3
1.4
1.5
Wavelength (μm)

CAPTION

Fig. 12.

Plot of $[\bar{\nu} - \bar{\nu}(SiO_2)]/v$ versus v for combination vibrations. The quantity $\bar{\nu}$ refers to combination vibrations which involve OH and SiO_2 components, whereas the quantity $\bar{\nu}(SiO_2)$ refers only to fundamental vibrations of SiO_2. The curved lines are from Fig. 8, components 1-4. The quantum number v refers only to OH vibrational levels -- not to levels of SiO_2. $\bar{\nu}(SiO_2) = 800\ cm^{-1}$ (⊛). Upper limit of error bar (Φ) refers to $\bar{\nu}(SiO_2) = 240\ cm^{-1}$ (Gaussian component value), whereas lower limit refers to $\bar{\nu}(SiO_2) = 280\ cm^{-1}$. For the combinations at 4100 cm^{-1} (⊡), 4520 cm^{-1} (◈), and 7920 cm^{-1} (X), the Raman $\bar{\nu}(SiO_2)$ values of 432, 1060, and 800 cm^{-1}, resp., were used, see Table I.

[ν̄ - ν̄(SiO2)]/ν, cm-1
3400
3600
3800
0
1
2
3
4
v
1
2
3
4

472:CAN:716:ddc
78u472-608

TECHNICAL REPORT DISTRIBUTION LIST, GEN

	No. Copies
Office of Naval Research Attn: Code 472 800 North Quincy Street Arlington, Virginia 22217	2
ONR Branch Office Attn: Dr. George Sandoz 536 S. Clark Street Chicago, Illinois 60605	1
ONR Area Office Attn: Scientific Dept. 715 Broadway New York, New York 10003	1
ONR Western Regional Office 1030 East Green Street Pasadena, California 91106	1
ONR Eastern/Central Regional Office Attn: Dr. L. H. Peebles Building 114, Section D 666 Summer Street Boston, Massachusetts 02210	1
Director, Naval Research Laboratory Attn: Code 6100 Washington, D.C. 20390	1
The Assistant Secretary of the Navy (RE&S) Department of the Navy Room 4E736, Pentagon Washington, D.C. 20350	1
Commander, Naval Air Systems Command Attn: Code 310C (H. Rosenwasser) Department of the Navy Washington, D.C. 20360	1
Defense Technical Information Center Building 5, Cameron Station Alexandria, Virginia 22314	12
Dr. Fred Saalfeld Chemistry Division, Code 6100 Naval Research Laboratory Washington, D.C. 20375	1

	No. Copies
U.S. Army Research Office Attn: CRD-AA-IP P.O. Box 1211 Research Triangle Park, N.C. 27709	1
Naval Ocean Systems Center Attn: Mr. Joe McCartney San Diego, California 92152	1
Naval Weapons Center Attn: Dr. A. B. Amster, Chemistry Division China Lake, California 93555	1
Naval Civil Engineering Laboratory Attn: Dr. R. W. Drisko Port Hueneme, California 93401	1
Department of Physics & Chemistry Naval Postgraduate School Monterey, California 93940	1
Dr. A. L. Slafkosky Scientific Advisor Commandant of the Marine Corps (Code RD-1) Washington, D.C. 20380	1
Office of Naval Research Attn: Dr. Richard S. Miller 800 N. Quincy Street Arlington, Virginia 22217	1
Naval Ship Research and Development Center Attn: Dr. G. Bosmajian, Applied Chemistry Division Annapolis, Maryland 21401	1
Naval Ocean Systems Center Attn: Dr. S. Yamamoto, Marine Sciences Division San Diego, California 91232	1
Mr. John Boyle Materials Branch Naval Ship Engineering Center Philadelphia, Pennsylvania 19112	1

TECHNICAL REPORT DISTRIBUTION LIST, 051A

	No. Copies
Dr. M.A. El-Sayed Department of Chemistry University of California, Los Angeles Los Angeles, California 90024	1
Dr. E. R. Bernstein Department of Chemistry Colorado State University Fort Collins, Colorado 80521	1
Dr. C. A. Heller Naval Weapons Center Code 6059 China Lake, California 93555	1
Dr. J. R. MacDonald Chemistry Division Naval Research Laboratory Code 6110 Washington, D.C. 20375	1
Dr. G. B. Schuster Chemistry Department University of Illinois Urbana, Illinois 61801	1
Dr. A. Adamson Department of Chemistry University of Southern California Los Angeles, California 90007	1
Dr. M. S. Wrighton Department of Chemistry Massachusetts Institute of Technology Cambridge, Massachusetts 02139	1
Dr. M. Rauhut Chemical Research Division American Cyanamid Company Bound Brook, New Jersey 08805	1
Dr. J. I. Zink Department of Chemistry University of California, Los Angeles Los Angeles, California 90024	1
Dr. D. Haarer IBM San Jose Research Center 5600 Cottle Road San Jose, California 95143	1
Dr. John Cooper Code 6130 Naval Research Laboratory Washington, D.C. 20375	1
Dr. William M. Jackson Department of Chemistry Howard University Washington, DC 20059	1
Dr. George E. Walraffen Department of Chemistry Howard University Washington, DC 20059	1

	No. Copies
Dr. Rudolph J. Marcus Office of Naval Research Scientific Liaison Group American Embassy APO San Francisco 96503	1
Mr. James Kelley DTNSRDC Code 2803 Annapolis, Maryland 21402	1